Novel monomers with N-methyl-D-glucamine segments and their application in structured porous materials for As capture

Daniele Caretti[1], Lorenzo Binda[1], Natalia Casis[2], Diana Estenoz[2]*

[1]Dipartimento di Chimica Industriale "Toso Montanari", University of Bologna, Viale Risorgimento 4, 40136 Bologna, Italy

[2]INTEC (Universidad Nacional del Litoral - Conicet), Güemes 3450, 3000 Santa Fe, Argentina

E-mail address: destenoz@santafe-conicet.gov.ar

ABSTRACT

The *N*-methyl-*D*-glucamine moieties exhibit high ability and selectivity towards arsenate ions in water by a complexation mechanism that involves their hydroxyl groups. In this work, the syntheses of two monomers containing *N*-methyl-*D*-glucamine, namely 4-vinylbenzyl-*N*-methyl-*D*-glucamine (VbNMDG) and *N*-methyl-*D*-glucamine methacrylamide (MNMDG) were studied. Different synthetic routes were considered in order to obtain liquid monomers able to polymerize and selectively capture arsenic. Furthermore, the incorporation of protective groups like trimethylsilyl moieties in the molecular structure was assessed to prevent transfer reaction during further polymerization. After polymerization, hydroxyl groups were deprotected using hydrofluoric acid. Following this methodology structured microporous polymeric films based on colloidal crystal templates were prepared. NMR and FTIR techniques were employed to follow the reactions and to determine the chemical structure of the obtained products. The morphology of materials was characterized by SEM.

The performances of the developed polymeric films to selectively capture arsenic was determined. Films showed an improved and reproducible sensitivity to arsenic detection exhibiting high values of arsenic capturing capability (around 90%).

1. Introduction

The presence of heavy metals such as Pb, Hg, Cd and As in water constitutes a major concern due to their bioaccumulation and their consequent adverse effects.[1] Among them, arsenic is one of the most significant toxic elements and its occurrence is undesirable in ground water for drinking purpose. The presence of arsenic in natural water sources is a consequence of both natural phenomena, such as erosion of arsenic-containing volcanic rocks, and anthropogenic causes, such as pollution from the mining industry.

Arsenic is mainly present in water as arsenate ions ($H_2AsO_4^-$ or $HAsO_4^{2-}$) As (V) and arsenite (H_3AsO_3) As (III) depending on various physicochemical conditions (pH, temperature, solution composition and redox potential).[2] However, arsenite is more mobile and toxic than arsenate and accounts for up to 60–99% of the total arsenic in water. Several studies show that arsenic poisoning is a serious threat to human health causing vomiting, abdominal pain, neurological disease, muscular weakness, skin and lung cancer.[3] A safe limit of arsenic concentration in drinking water has been recommended by the World Health Organization to be set at 10 μg L^{-1} but in some geographical areas, like South America, the amount of arsenic in water is particularly high causing various severe pathologies.[4] For this reason, both sensing and selective arsenic removal from water is crucial. Extensive researches are being carried out to develop methods that can unambiguously quantify concentrations of arsenic species at ultra-trace level as well as viable technologies for economic and effective remediation of arsenic species in water reservoirs.

Traditional techniques for the removal of heavy metals involve several categories such as absorption and ion exchange, oxidation, coagulation-flocculation, biological methods and membrane technologies.[1,5-9] In particular, for arsenic removal, the efficacies depend on the types and concentrations of As species, the pH, the presence of other dissolved ions and the volume of water to be treated. In addition, many arsenic elimination technologies are more effective to extract pentavalent arsenic than the trivalent form, and multiple steps (such as pre-oxidation, coprecipitation and filtration) may be required to achieve treatment goals.[10-13] The limitations of these procedures are the high investment cost and management of the installations and the difficulty in maintaining the continuity of exercise necessary for the removal efficiency.

Regarding the quantification and sensing of arsenic in real samples, nanomaterials based on colorimetric, electrochemical and Raman spectroscopy techniques among others, were proposed for kits development.[14] Many efforts have already been made toward elaborate portable sensors, but unfortunately, most of these are able to detect only free ions as they are present in artificial matrices and not in the form of metal–organic complexes as they are in real samples. As a result, a pretreatment of samples becomes also necessary. This is a major drawback towards implementing sensors in the field for real-time detection. Another issue to consider is the possibility of sensor malfunction due to the simultaneous presence of chemical and biological species that can be found in real samples and also to the insufficient amount of analytes that requires preconcentration techniques.[15] Successful strategies to address these concerns will result in highly selective, sensitive, and reproducible sensing devices for real samples.

Several amino-functional substrates able to remove heavy metal from water have been studied.[16-21] Particularly, *N*-methyl-*D*-glucamine (NMDG) (Figure 1) is well known for its high affinity for borate ion under alkaline conditions.[22] In several studies, it was found that

NMDG also exhibited high affinity and selectivity for arsenate ions in aqueous solutions at neutral or acidic pH.[23-27] Dambies et al.[23] investigated the functionalization by NMDG of a preformed resin for the removal of arsenate from an aqueous solution containing also other ions (sulfate, phosphate and chloride). The results showed a very good performance to selectively remove arsenic because the complexation was unaffected by the presence of these interferences. Besides, the NMDG resin showed no affinity for arsenate when the solution pH exceeded 9.0, indicating that it can be regenerated with alkaline solution after arsenate loading. It was proved that the key variable in NMDG selectivity is that the resin has to be protonated prior to contact with the aqueous solution: indeed, the sorbitol moiety forms a stable complex with As (V) in acid media. Unfortunately, this functionalization procedure does not allow to obtain a well-defined polymer structure because the functionalization reaction is not exhaustive. As far as the authors know, direct polymerization of the proper functionalized monomers is not reported.

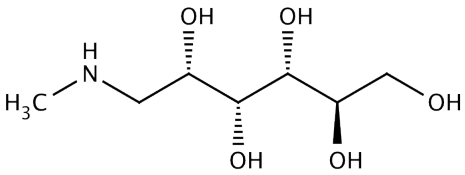

Figure 1. *N*-methyl-*D*-glucamine.

In order to increase the detection limits of some contaminants, many researchers have proposed an effective method that involves colloidal crystal templates made with silica particles and inverse opal technique to prepare polymers with 3D, highly ordered and microporous structures able to detect organic compounds (like atrazine, testosterone and bisphenol A) in aqueous solution by rapid assay.[28-30] The procedure involves the infiltration of the reaction mixture (monomers, initiator, solvent) into the interspaces of the colloidal crystal followed by polymerization. Then, the removal of template provides the 3D-ordered structure with a perfect control of the film morphology. These opal photonic crystals can be used to

fabricate chemical sensors since they exhibit the ability to swell or shrink in water upon molecular recognition or environmental conditions leading to a change in their optical properties (i.e.: reflectance). Moreover, the high sensitivity and specificity observed in these polymeric systems is mainly due to the high surface-to-volume ratio of the structure that allow for a more efficient mass transport in submicrometer-sized pores and enhance surface reactions.[30,31]

In this work, the synthesis and characterization of two novel monomers containing *N*-methyl-*D*-glucamine segments are studied: 4-vinylbenzyl-*N*-methyl-*D*-glucamine (VbNMDG) and *N*-methyl-*D*-glucamine methacrylamide (MNMDG) derivatives. Different synthetic strategies are implemented in order to obtain functionalized liquid monomers able to be infiltrated into colloidal crystal templates. Films with microporous ordered structures are prepared and the arsenate ion capture performance is determined using atomic absorption spectroscopy technique. The main aim is to design high specific surface area materials with low arsenic detection limits.

2. Materials and Methods

N-methyl-*D*-glucamine, 4-vinylbenzyl chloride, methacryloyl chloride, azo-bis-isobutyronitrile (AIBN), 1,4-divinylbenzene (DVB), hydrofluoric acid, methanol, HNO_3, $Na_2HAsO_4.7H_2O$, Na_2CO_3 and KOH were provided by Sigma Aldrich (Italy) at reagent grade and they were used without further purification. THF was distilled on Na/benzofenone. Deionized water was used to prepare all the aqueous solutions.

A Varian Unicam Solaar 969 atomic absorption spectrometer working at 193.7 nm with a bandwidth of 0.7 nm was employed for arsenic quantification. The pH meter used was a 330 Inolab WTW. For Dynamic Light Scattering (DLS) a Malvern Nanosizer 2000 was employed. SEM measurements were carried out by a JEOL JSM-840A equipment. A Perkin Elmer 1750

FT-IR spectrometer was used and NMR spectra were recorded by a Varian “Mercury 400” spectrometer operating at 400 MHz.

3. Experimental Work

3.1. Synthesis and Characterization of Monomers Functionalized with *N*-methyl-*D*-glucamine

Two different monomers, 4-vinylbenzyl-*N*-methyl-*D*-glucamine (VbNMDG) and *N*-methyl-*D*-glucamine methacrylamide (MNMDG) having all hydroxyls protected by trimethylsilane groups were synthesized. In both synthetic procedures, the following two stages were involved: i) the linking of *N*-methyl-*D*-glucamine moiety on styrenic or methacrylic monomers, and ii) the protection of the hydroxyl groups present in the *N*-methyl-*D*-glucamine moiety with trimethylsilane (TMS).

3.1.1. Synthesis of 4-vinylbenzyl-N-methyl-D-glucamine (VbNMDG)

N-methyl-D-glucamine (9.7 g, 50.0 mmol) was suspended in 200 ml of methanol and an equimolar amount of 4-vinylbenzyl chloride (7.63 g, 50.0 mmol) dissolved in methanol was incorporated to the solution. Anhydrous Na_2CO_3 was then added in the same molar ratio (50 mmol) (Figure 2).

The reaction proceeded under vigorous stirring for 3 h at room temperature. The mixture was filtered and dried to evaporate the methanol. The product obtained was purified by crystallization in chloroform and characterized by NMR. Yield 13.5 g (87%).

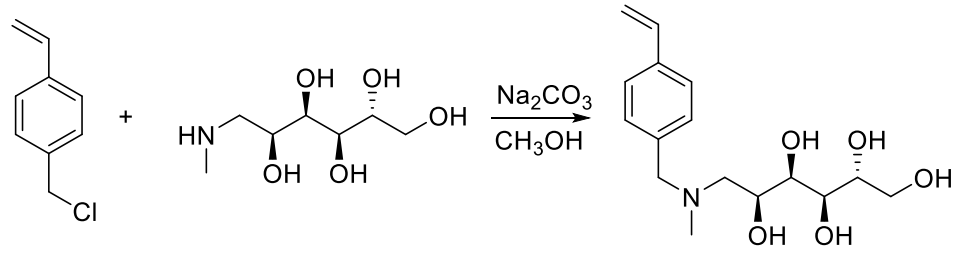

Figure 2. Synthesis of 4-vinylbenzyl-*N*-methyl-*D*-glucamine.

^{1}H-NMR (400 MHz, in $(CD_3)_2SO+D_2O$) [ppm referred to TMS]

2.10 (s, 3H, N-CH_3); 2.4 – 2.6 (m, 2H, N-C**H$_2$**-CH); 3.30 – 3.85 (m, 8H, CH + Ar-CH_2-N + C**H$_2$**-OH); 5.20 (dd, 1H, CH=C**H**$_2$ cis); 5.85 (dd, 1H, CH=C**H**$_2$ trans); 6.70 (dd, 1H, C**H**=CH_2); 7.35 (dd, 4H, CH aromatic).

3.1.2. Synthesis of N-methyl-D-glucamine Methacrylamide (MNMDG)

N-methyl-*D*-glucamine (5 g, 25.6 mmol) was dissolved in 120 mL of methanol and 15 mL of water. The solution was placed in a flask into an ice bath and methacryloyl chloride (2.67 g, 25.6 mmol) dissolved in THF was added drop by drop (Figure 3).

The reaction mixture was stirred for an hour keeping the pH = 8-9 by using KOH 2 M. Then, the mixture was dried by solvent evaporation. The product was purified by crystallization in ethanol and then characterized by NMR. Yield 5.7 g (85%).

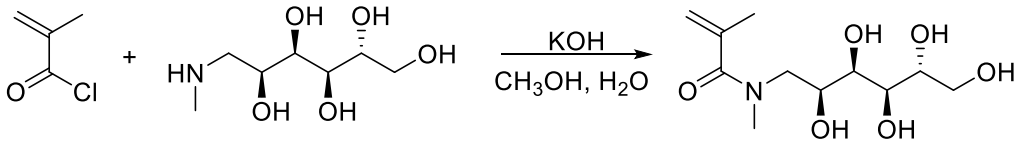

Figure 3. Synthesis of *N*-methyl-*D*-glucamine methacrylamide.

^{1}H-NMR (400 MHz, in $(CD_3)_2SO+D_2O$) [ppm referred to TMS]

1.80 (s, 3H, CH_2=C-C**H$_3$**); 2.90 (s, 3H, N-CH_3); 3.25 - 3.65 (m, 8H, CH + CH_2); 5.05 (d, 2H, CH_2=C).

3.1.3 Protection of the Hydroxyl Groups of the N-methyl-D-glucamine Moieties with Trimethylsilane Groups (TMS)

In order to prevent transfer reactions during further polymerizations due to the presence of hydroxyl groups in both monomers, OH groups were protected following these procedures:

a) 4-vinylbenzyl-*N*-methyl-*D*-glucamine (5.0 g, 16.0 mmol) was dissolved in anhydrous THF in a three necked round bottom flask. The reaction was carried out with an excess of trimethylsilyl chloride (TMSC) and using triethylamine (TEA) in equimolar amounts to the TMSC (Figure 4).

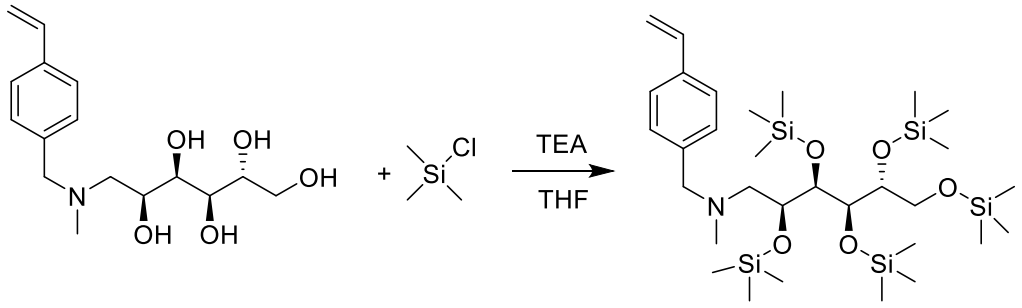

Figure 4. Protection of 4-vinylbenzyl-*N*-methyl-*D*-glucamine with TMSC.

The reaction proceeded under nitrogen atmosphere for 3 h. The protection progress was monitored by IR spectroscopy. The reaction mixture was filtered off and the solvent and unreacted volatile products were removed by vacuum. The viscous liquid obtained was dissolved in 10 mL of ethyl ether and washed with water (5 × 10 mL). After drying the organic phase with anhydrous sodium sulfate and solvent removal, a viscous liquid was obtained and characterized by NMR. Yield 8.1 g (75%).

^{1}H-NMR (400 MHz, in $CDCl_3$) [ppm referred to TMS]

0.05 - 0.15 (m, 45H, Si-CH_3); 2.05 (s, 3H, N-CH_3); 2.4 – 2.6 (m, 2H, N-C**H$_2$**-CH); 3.40 – 4.00 (m, 8H, CH + Ar-CH_2-N + CH_2-O); 5.2 (dd, 1H, CH=C**H**$_2$ cis); 5.75 (dd, 1H, CH=C**H$_2$** trans); 6.70 (dd, 1H, C**H**=CH_2); 7.30 (m, 4H, CH aromatic).

^{13}C-NMR (400 MHz, in $CDCl_3$) [ppm referred to $CDCl_3$]

-0.5 - 1 (15C, Si-CH_3); 42.8 (1C, N-CH_3); 59.9, 63.0, 63.6 (3C, CH_2); 73.1, 74.9, 75.2, 77.1 (4C, CH); 112.9 (1C, CH=**C**H_2); 126.0, 129.0 (4C, CH aromatic) 136.1 (1C, **C**H=CH_2), 136.6, 139.3 (2C, quaternary aromatic).

b) *N*-methyl-*D*-glucamine methacrylamide (1 g, 3.8 mmol) was dissolved in pyridine in a three necked round bottom flask. The reaction was carried out by adding an excess of trimethylsilyl chloride (TMSC) and hexamethyldisilazane in 1:1 ratio (Figure 5).

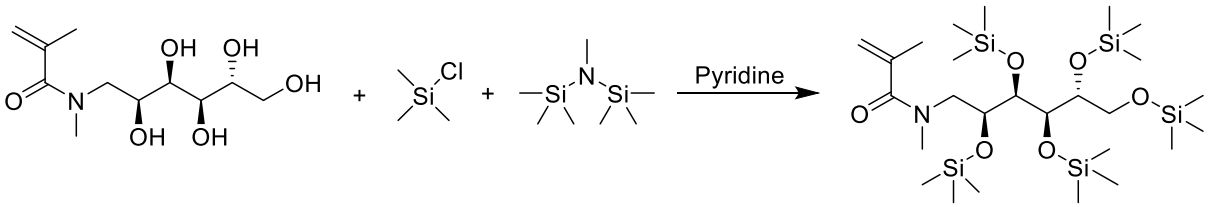

Figure 5. Protection of *N*-methyl-*D*-glucamine methacrylamide with TMSC.

The reaction proceeded under nitrogen atmosphere for 10 minutes and its progress was followed by IR spectroscopy. The mixture was filtered and the solvent eliminated. The raw product was dissolved in diethyl ether and washed with some fractions of water. The ethereal phase was finally evaporated and the product characterized by NMR. Yield 1.65 g (80%). The product obtained was a viscous liquid.

^{1}H-NMR (400 MHz, in $CDCl_3$) [ppm referred to TMS]

0.0 - 0.2 (m, 45H, Si-CH_3); 1.85 (s, 3H, CH_2=C-C**H$_3$**); 2.95 (s, 3H, N-C**H$_3$**); 3.50 – 4.0 (m, 8H, CH + CH_2); 5.1 (d, 2H, CH_2=C).

^{13}C-NMR (400 MHz, in CDCl3) [ppm referred to $CDCl_3$]

-1 – 1 (15C, Si-CH_3); 21.0 (1C, CH_2=C-**C**H_3); 32.0 (1C, N-CH_3); 52.0 – 77.0 (6C, CH + CH_2); 115.0 (1C, CH_2=**C**H); 140.0 (1C, CH_2=**C**); 173.0 (1C, C=O).

FT-IR (υ in cm^{-1})

2957 (stretch C-H); 1650 (stretch C=O ammidic); 1089 (stretch C-O); 885 (bend R_2C=CH_2).

3.2. Polymerization of 4-vinylbenzyl-*N*-methyl-*D*-glucamine and *N*-methyl-*D*-glucamine Methacrylamide Derivatives

The bulk polymerization of both protected monomers was carried out using azo-bis-isobutyronitrile, AIBN (2% mol) as thermal initiator and 1,4-divinylbenzene (DVB) (4%, respect to silylated monomer) as crosslinking agent. Mixtures were degassed for 10 min with nitrogen and kept for 4 h under a nitrogen atmosphere at 110 °C. Polymers obtained were washed with dioxane and distilled water, and subsequently dried in an oven at 50 °C. Products were characterized by IR. Finally, polymers were treated with HF solution (5%) stirring for 5-10 minutes to deprotect the OH groups and then, they were again analyzed by IR in order to check the deprotection efficiency.

3.3. Fabrication and Characterization of Microporous Films for Retaining Arsenic

3.3.1. Synthesis of Colloidal Crystal Template and Films

Microporous films were fabricated from templates made of silica particles. The synthesis of silica particles and colloidal crystals was carried out following the procedure described in Casis et al.[32] Briefly, the monodisperse particles were synthesized following the Stöber method.[33] TEOS (11 mL) and ethanol (210 mL) were mixed in a flask and stirred. Ammonia concentrated solution (11 mL) and deionized water (17 mL) were introduced and allowed to react for 4 h. Then, additional 11 mL of TEOS and 10 mL of water were added to the flask again stirred for 4 h to allow further reaction. The suspension was centrifuged and redispersed in ethanol three times to completely wash the particles. A cleaned glass slide was vertically placed into a flask containing silica particles suspended in ethanol and after the volatilization of ethanol, the colloidal crystals formed on both side of the slide.

To obtain the films, four different mixtures were prepared using only protected VbNMDG monomer. DVB was added as crosslinker, and AIBN (2% mol respect to monomers) as thermal initiator (see Table 1).

Table 1. Composition of Polymerization Mixtures

Mixture	Monomer	DVB (% mol respect to protected VbNMDG)
1	Protected VbNMDG	4
2	Protected VbNMDG	8
3	Protected VbNMDG	16
4	Protected VbNMDG	32

The procedure for films fabrication is shown in Figure 6. The homogeneous mixtures were added dropwise on silica colloidal crystals deposited on a glass slide. Another slide was place upon the colloidal crystals film and the two slides held together to retain the above-mentioned mixture, forming a "sandwich" structure (Figure 6c).

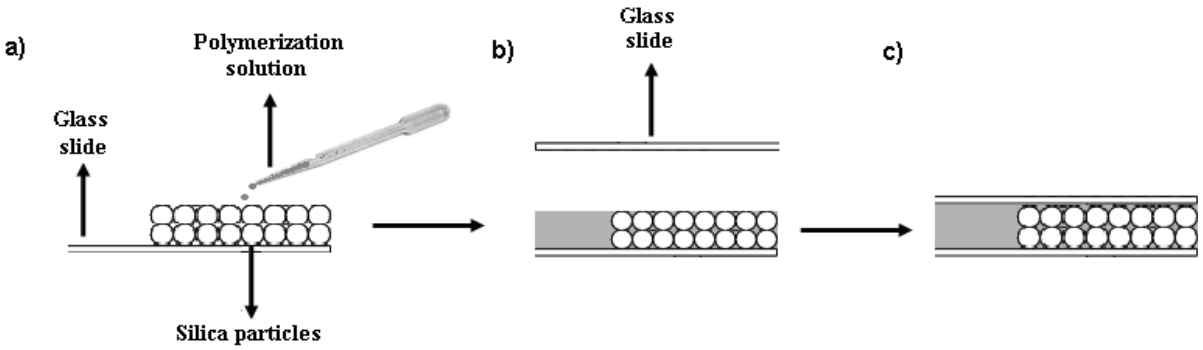

Figure 6. Infiltration (a,b) and polymerization process (c). Reproduced with permission.[32]

Polymerizations were carried out at T = 110 °C. Then, silica particles were removed by immersing the system for 12 h in 5% hydrofluoric acid solution. Finally, the resulting polymer films were washed with distilled water.

3.3.2. Characterization of Silica Particles and Films

Particle size of the synthesized silica and their distribution were determined by Dynamic Light Scattering. Silica particles and porous films were also analyzed by Scanning Electron Microscopy (SEM) to measure the particles and the pore size as well observing their morphology. Samples were attached to a metal mount using carbon tape and were coated with

a thin layer of gold to provide a conductive surface using a sputter coater (CRC-100). Quantitative analysis of the images was done using ImageJ software (National Institutes of Health, NIH).

3.4. Evaluation of Microporous Films for the Arsenic-capturing Capability

The arsenic capturing capability was evaluated following the procedure reported by Urbano et al.,[25] including batch equilibrium experiments. All tests were carried out in a test tube using 30 mg of polymer and 10 mL of a prepared arsenate solution (200 mg L^{-1}) at pH 6 adjusted by adding 0.1 M HNO_3. At pH 6, the major amount of arsenate exists in the monovalent form $H_2AsO_4^-$, and based on previous literature results, it has been demonstrated that sorption is favored.[25,27] After 24 h stirring, polymers were filtered off, washed and then, the solution was transferred to 50 mL calibrated flask. The arsenic concentration in the filtrate was measured by atomic absorption spectroscopy. A prepared solution of 500 mg L^{-1} of $Na_2HAsO_4.7H_2O$ was used for calibration.

The arsenic capturing capability (As(V) capture, %) was calculated from the following equation:

$$\text{As(V) capture} = \left(1 - \frac{C_e}{C_i}\right) 100\% \quad (1)$$

where C_i and C_e are the initial and the equilibrium concentrations of the arsenic in solution (in mg mL^{-1}), respectively.

4. Results and Discussion

The styrenic monomer 4-vinylbenzyl-*N*-methyl-*D*-glucamine was obtained by reacting *N*-methyl-*D*-glucamine and 4-vinyl-benzyl-chloride in the presence of sodium carbonate as described in the Experimental Part (section 3.1.1, Figure 2). The monomer was solid, so the

infiltration into colloidal crystal for bulk polymerization was not possible. A second step was therefore necessary not only to obtain a viscous liquid monomer but also to protect the hydroxylic groups of the monomer that can act as transfer agents during the polymerization. For this purpose, a classical protection with trimethylsilyl groups from trimethyl-silyl-chloride was carried out (Figure 4). The procedure was previously described in the Experimental Part. Although pyridine is frequently employed for this type of reaction, it exhibits problems related to its removal from an oily product in the purification stage. For this reason, TEA was chosen to neutralize the hydrochloric acid produced during the reaction that took 3 h and was followed by IR. The end was reached when the IR spectrum detected the absence of the –OH characteristic band (3650-3590 cm^{-1}). The resulting monomer was in a liquid state.

The NMR spectra of the product showed in Figure 7 and 8 indicate total protection of the hydroxyl groups.

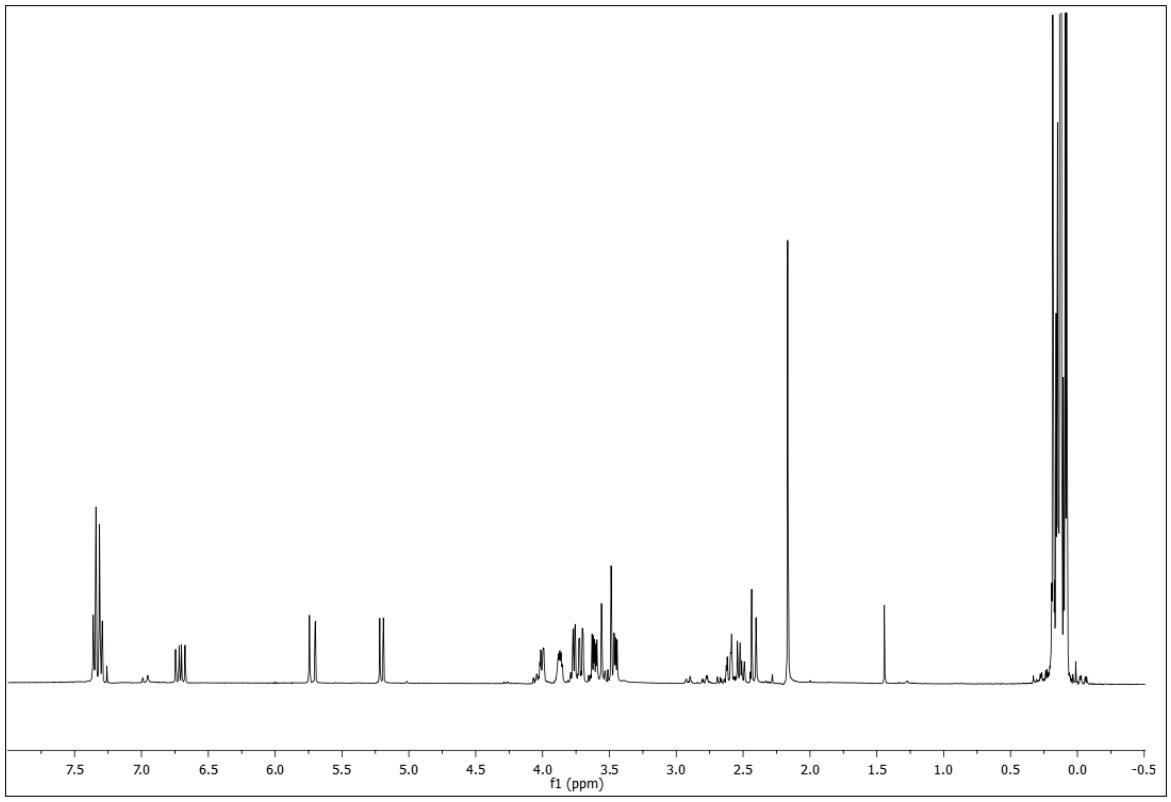

Figure 7. ^{1}H-NMR Spectrum of VbNMDG protected with TMS in $CDCl_3$.

In particular, from the ^{13}C-NMR spectrum (Figure 8), it can be observed that there are 5 signals between 1 and -0.5 ppm which are ascribable to the 5 protecting groups linked to the molecule, confirming the successful protection of all hydroxyl groups.

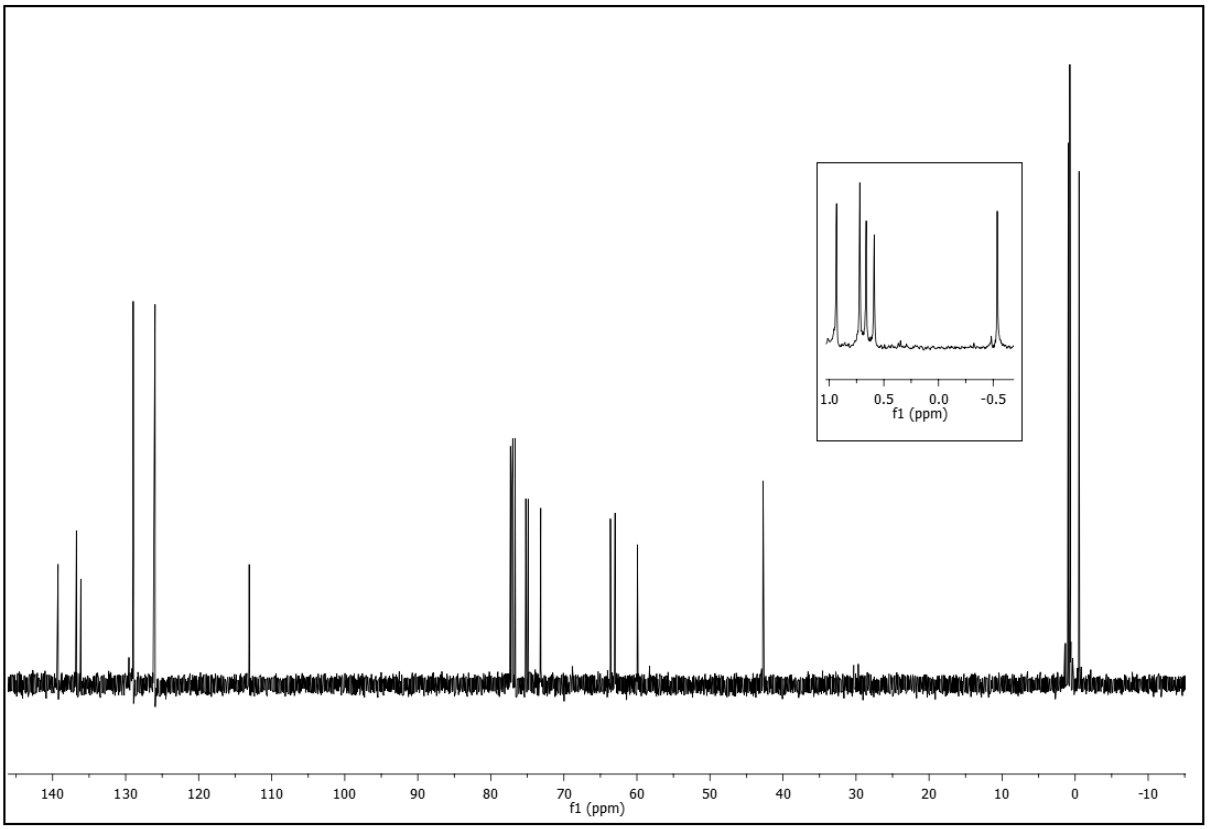

Figure 8. ^{13}C-NMR Spectrum of VbNMDG protected with TMS in $CDCl_3$

An alternative order of reaction procedure was also considered: the protection of the hydroxyl groups of *N*-methyl-*D*-glucamine and the subsequent reaction with 4-vinyl-benzyl-chloride but the resulting overall yield was lower.

As described in the Experimental Part (section 3.1.2), the *N*-methyl-*D*-glucamine methacrylamide was obtained by reacting *N*-methyl-*D*-glucamine and methacryloyl chloride in aqueous media. The HCl by-product of the reaction was neutralized with a KOH solution. The monomer obtained was solid, and as in the previous case, the protection with trimethylsilyl functionalities was carried out. Differently from the previous case,

trimethylsilyl chloride alone is not able to react with all hydroxyl groups and the addition of hexamethyldisilazane and pyridine was necessary as it was indicated.

Even adopting these reaction conditions, the presence of some hydroxyls (slight peak at 3434 cm^{-1} in the IR spectra) was still observed. On the other hand, by extending the reaction time for a further 30 min no variation on the peak intensity was observed. The effective protection of OH groups can be quantified by ^{1}H-NMR analyses but is not a relevant issue because the obtained product is in the liquid state and the protective groups will be subsequently removed after polymerization. Anyway ^{13}C-NMR spectrum was presented in Figure 9. The presence of 5 different peaks in the range from 1 to -1 ppm attributable to the 5 TMS groups inserted into the molecule indicate a good protection.

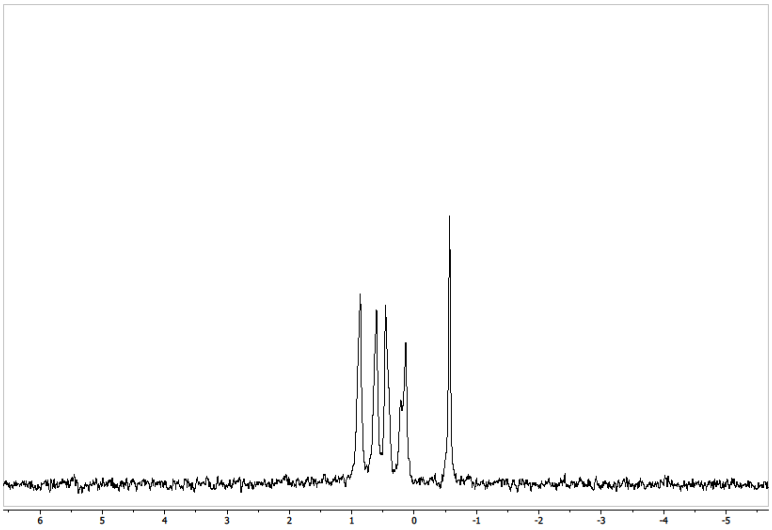

Figure 9. Portion of ^{13}C-NMR spectrum of MNMDG protected with TMS groups, in $CDCl_3$.

The bulk polymerization of VbNMDG protected with TMS was carried out in the presence of a crosslinking agent (section 3.2) followed by HF treatment. The IR analysis confirmed its deprotection (Figure 10, presence of OH groups at 3390 cm^{-1}).

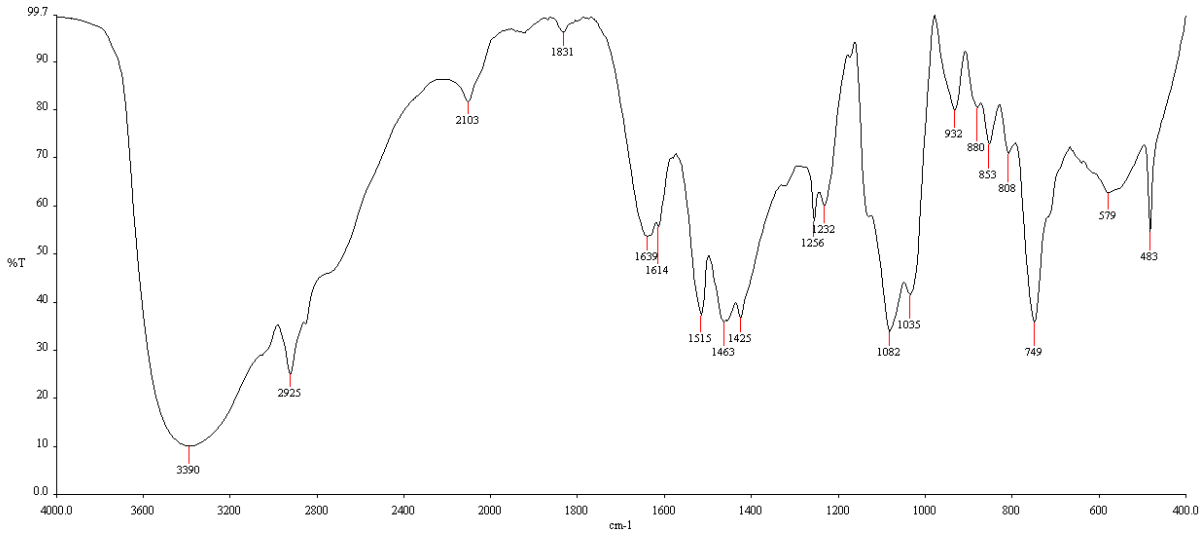

Figure 10. FT-IR Spectrum of the polymerized VbNMDG crosslinked with 1,4-DVB.

For *N*-methyl-*D*-glucamine methacrylamide protected with TMS, the polymerization was unfortunately not effective. After 3 hours of reaction a slight coloration was observed. After 5 hours no further changes in the appearance of the product were observed and it was decided to stop the heating. The product was soluble in chloroform indicating the absence of crosslinking and from the NMR spectrum it was evident that polymerization has failed, since at 5.1 ppm there are still evident signals characteristic of the methacrylic double bond that it would not have been detected in the case of successful polymerization. Probably, the lack of polymerization may be due to the presence, although in small amounts, of impurities, which are difficult to remove from the oily monomer interfering in the polymerization process. Indeed, trimethylsilyl derivatives are normally characterized by a certain sensitivity to hydrolytic conditions that associated to the consistency of the product has limited the possibility of efficient purification. For this reason, only the VbNMDG protected monomer was considered for the further fabrication of microporous films.

The characterization of silica produced particles was carried out by DLS and SEM (Figure 11) and the sizes obtained were 274 ± 4 nm and 263 ± 15 nm, respectively, showing a good agreement between results from both techniques. A slightly higher value obtained with the

DLS method may be attributed to the hydrodynamic radius of silica particles, which eventually includes solvating molecules. Contrarily in SEM measurements performed under vacuum, the elimination of the retained water can be expected.

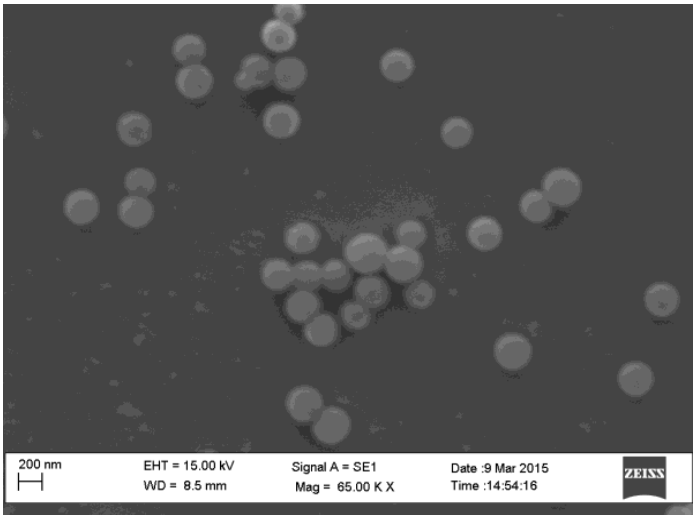

Figure 11. SEM micrograph of silica particles.

Polymeric films were obtained as described in the Experimental part (section 3.3.1) using VbNMDG and DVB. The further characterization by SEM shows that the membrane surface appears quite homogeneous (Figure 12a) whereas the cavities of the internal porosity presented a size proportional to the silica particles used for the film's synthesis (Figure 12b). The mean effective pore size of film derived from the contact points between the particles in the deposit has a resulting value of 87 nm.

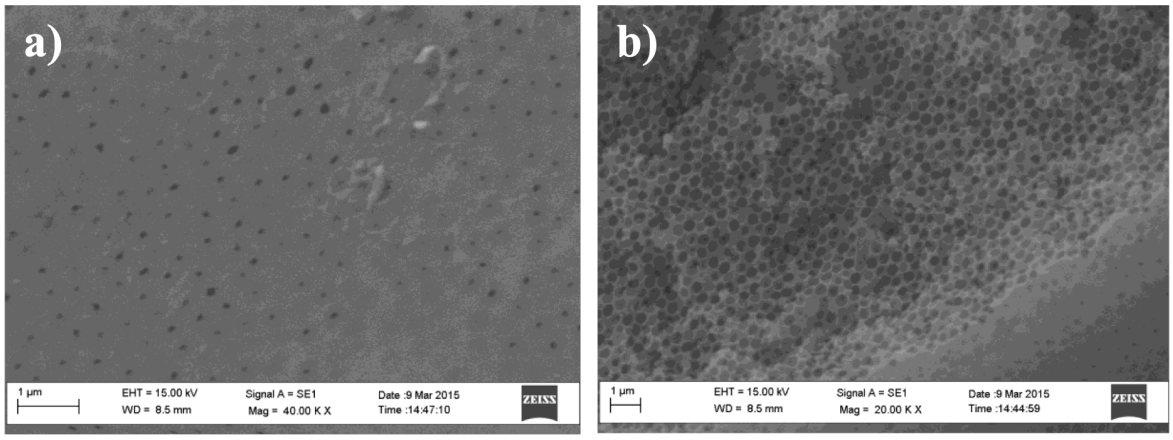

Figure 12. SEM micrographs of porous films. a) top view and b) cross section.

Porous polymeric samples synthesized with different monomer ratio (VbNMDG:DVB) were evaluated and different As(V) capture values were obtained. As shown in Table 2, the amount of arsenic captured decreases with the increase of crosslinking degree as a consequence of the reduced arsenic diffusion in the polymer matrix and the limited mobility of the hydroxyls groups, responsible of the complexation mechanism. As expected, the apparent mechanical strength increased with the crosslinking degree in the studied monomer ratio range. The highest capture value was achieved for a 4% molar ratio of DVB and it was similar to those reported in the literature.[23,26] Apart the higher arsenic capture capability this membrane also possesses an adequate mechanical strength for practical application.

Table 2. As(V) Capture Values (%)

Membrane DVB % content (mol)	As(V) capture %
4	89
8	70
16	55
32	47

5. Conclusions

The synthesis of two monomers functionalized with *N*-methyl-*D*-glucamine, and their application for the preparation of novel microporous materials able to capture arsenic were investigated.

Different methods of synthesis were experimentally studied to obtain the monomers 4-vinylbenzyl-*N*-methyl-*D*-glucamine and *N*-methyl-*D*-glucamine methacrylamide protected with trimethylsilyl groups. Methacrylamide derivative was not able to polymerize probably

due to its lack of purity. In contrast, styrenic monomer polymerization was successfully carried out.

Silica nanoparticles were synthesized and deposited on a glass support for the construction of a template using the self-assembling technique, VbNMDG protected monomer, AIBN and DVB were infiltrated and subsequently polymerized, yielding good results and reproducibility.

Porous polymeric samples synthesized with different monomer ratio VbNMDG:DVB and their subsequent deprotection in 5% HF were finally evaluated for the arsenic (V) capture. The results were comparable to the literature values.[23,26]

The novel material has potentiality for the development of membranes able to efficiently remove arsenic (V) as well as highly sensitive portable sensors applied for the analysis of real environmental samples for arsenic quantification in water. To the latter application, the shift of the Bragg diffraction peak associated to the photonic structure would allow detecting and quantifying very low concentrations of As.

Acknowledgements

To CONICET, MINCyT and Universidad Nacional del Litoral for funding.

References

[1] R. K. Gautam, S. K. Sharma, S. Mahiya, M. C. Chattopadhyaya, in *Heavy Metals In Water: Presence, Removal and Safety*, DOI: 10.1039/9781782620174-00001*e*ISBN: 978-1-78262-017-4, **2014**, Ch. 1.
[2] P. L Smedley, D. G. Kinniburgh *Appl. Geochemistry* **2002**, *17*, 517.
[3] WHO in: Arsenic in Drinking Water. Organisation W.H., editor, WHO, Geneva, Switzerland, **2011**.
[4] G. Howard, Arsenic, drinking-water and health risk substitution in arsenic mitigation: a discussion paper, World Health Organization, **2003**.
[5] T. S. Y. Choong, T. G. Chuah, Y. Robiah, F. L. G. Koay, I. Azni *Desalination* **2007**, *217,* 139.
[6] D. Mohan, C. U. Pittman *J. Hazard. Mater*. **2007**, *142*, 1.
[7] R. Johnston, H. Heijnen, **2015**, available online: http://archive.unu.edu/env/Arsenic/Han.pdf.
[8] M. Shih *Desalination* **2005**, *172*, 85.
[9] J. Sánchez, B. L. Rivas *Desalination* **2011**, *270 (1–3)*, 57.
[10] N. Ricci Nicomel, K. Leus, K. Folens, P. Van Der Voort, G. Du Laing *Int. J. Environ. Res. Public. Health* **2016**, *13*, 1.

[11] M. L. Chen, L. Y. Ma, X. W. Chen *Talanta* **2014**, *125*, 78.
[12] M. M. Nearing, I. Koch, K. J. Reimer *Spectrochim. Acta - Part B At. Spectrosc*. **2014**, *99*, 150.
[13] R. Singh, S. Singh, P. Parihar, V. P. Singh, S. M. Prasad *Ecotoxicol. Environ. Saf.* **2015**, *112*, 247.
[14] D. Melamed *Anal. Chim. Acta* **2005**, *532 (1),* 1.
[15] N. Sinha, *IEEE Nanotechnology Magazine* **2014**, 17.
[16] H. T. Ha, N. T. Huong, L. L. Dan, N. D. Tung, V. B. Trung, T. D. Minh. *Hindawi, Journal of Analytical Methods in Chemistry* **2020**, *2020*, 1.
[17] H. T. Ha, T. D. Minh, H. M. Nguyet *VNU Journal of Science: Earth and Environmental Sciences* **2121**, *37*, 61.
[18] H. T. Ha, N. T. Huong, T. D. Minh, B. Lee, E. R. Rene, T. V. B. Linh, H. D. Minh, N. N. Quang, P. C. Mai, N. Q. Duc *J. Environ. Eng.* **2020**, *146 (7),* 04020060.
[19] Z. Dousti, L. Dolatyari, M. R. Yaftian, S. Rostamnia *Separation Science and Technology* **2018**, *54*, 2609.
[20] L. Dolatyari, M. R. Yaftian, S. Rostamnia *Separation Science and Technology* **2016**, *169*, 8.
[21] L. Dolatyari, M. Shateri, M. R. Yaftian, S. Rostamnia *Separation Science and Technology* **2017**, *52*, 393.
[22] S. D. Alexandratos *J. Hazard. Mater*. **2007**, *139*, 467.
[23] L. Dambies, R. Salinaro, S. D. Alexandratos *Environ. Sci. Technol.* **2004**, *38*, 6139.
[24] B. F. Urbano, B. L. Rivas, F. Martinez, S. D. Alexandratos *Chem. Eng. J.* **2012**, *193/194*, 21.
[25] B. F. Urbano, B. L. Rivas, F. Martinez, S. D. Alexandratos *React. Funct. Polym.* **2012**, *72 (9)*, 642.
[26] L. Toledo, B. L. Rivas, B. F. Urbano, J. Sánchez *Sep. Purif. Technol*. **2013**, *103*, 1.
[27] Y. T. Wei, Y. M. Zheng, J. P. Chen *J. Colloid Interf. Sci*. **2011**, *356*, 234.
[28] J. Y. Chul, J. Y. Park *ACS Appl. Mater. Interfaces* **2016**, *8*, 7381.
[29] A. J. Kadhem, S. Xiang, S. Nagel, C. Lin, M. M. Fidalgo de Cortalezzi *Polymers* **2018**, *10*, 349.
[30] Q. Yang, X. Wu, H. Peng, L. Fu, X. Song, J. Li, H. Xiong, L. Chen *Talanta* **2018**, *176*, 595.
[31] X. Hu, G. Li, M. Li, J. Huang, Y. Li, Y. Gao, Y. Zhang *Adv. Funct. Mater.* **2008**, *18*, 575.
[32] N. Casis, S. Ravaine, S. Reculusa, V. L. Colvin, M. R. Wiesner, D. A. Estenoz, M. M. Fidalgo de Cortalezzi *Macromol. React. Eng*. **2010**, *4*, 445.
[33] W. Stöber, A. Fink, E. Bohn *J. Colloid Interface Sci.* **1968**, *26*, 62.